Colloid Polym Sci (2004) 282: 1347–1358
DOI 10.1007/s00396-003-1036-5

ORIGINAL CONTRIBUTION

Chin-Ping Yang
Hsun-Ching Chiang

Organosoluble and light-colored fluorinated polyimides based on 9,9-bis[4-(4-amino-2-trifluoromethylphenoxy)phenyl]fluorene and aromatic dianhydrides

Received: 4 July 2003
Accepted: 14 November 2003

C.-P. Yang (✉) · H.-C. Chiang
Department of Chemical Engineering,
Tatung University, 40 Chungshan North
Road, 3rd Section, 104 Taipei, Taiwan
E-mail: cpyang@ttu.edu.tw
Tel.: +886-2-25925252 (ext. 2977)

Abstract A novel fluorinated diamine monomer, 9,9-bis[4-(4-amino-2-trifluoromethylphenoxy)phenyl] fluorene (**II**) was prepared via the nucleophilic substitution reaction of 2-chloro-5-nitrobenzotrifluoride with 9,9-bis(4-hydroxyphenyl)fluorene in the presence of potassium carbonate, followed by catalytic reduction with hydrazine and Pd/C. Polyimides **V** were synthesized from diamine**II** and various aromatic dianhydrides$\mathbf{III_{a\text{-}f}}$ via thermal imidization. These polymers had inherent viscosities ranging from 0.84 to 1.03 dL/g and were soluble in a variety of organic solvents such as NMP, DMAc, DMF, and DMSO, and some could even be dissolved in less polar solvents such as *m*-cresol, pyridine, and dioxane. Polyimide films $\mathbf{V_{a\text{–}f}}$ had tensile strengths of 85–105 MPa, elongations to break of 7–9%, and initial moduli of 2.13–2.42 GPa. The glass transition temperature of these polymers were in the range of 277–331 °C, their 10% weight loss temperatures were in the range of 539–594 °C in nitrogen and above 544 °C in air, and their char yields at 800 °C in nitrogen ranged between 55–65 wt%. Compared with nonfluorinated polyimides**VI**, **V** showed better solubility and lower color intensity. Low dielectric constants (2.68–2.85 at 1 MHz) and low moisture absorptions (0.12–0.24 wt%) were also observed. In particular, $\mathbf{V_{c\text{-}f}}$ afforded lightly-colored films, which had cutoff wavelengths lower than 385 nm and *b** values ranging from 6 to 22.

Keywords 9,9-bis[4-(4-amino-2-trifluoromethylphenoxy)phenyl] fluorene · Light-colored · Organosoluble

Introduction

Aromatic polyimides are well-known as high performance polymer materials due to their excellent thermal stabilities and balanced mechanical and electric properties [1, 2, 3, 4, 5, 6, 7]. Polyimides are mainly used in the aerospace and electronics industries in the form of films and moldings. The optical transparency of polyimide films is of special importance in some applications, such as flexible solar radiation protectors [8], orientation films in liquid crystal display devices [9], optical waveguides for communication interconnects [10], and optical half-waveplates for planar lightwave circuits [11]. However, the wholly aromatic polyimides strongly absorb in the visible region of their UV-visible spectra and are pale yellow or deep reddish yellow because of their highly conjugated aromatic structures and/or the intermolecular charge-transfer complex (CTC) formation; besides, they are difficult to process because of high softening temperatures and limited solubility in commercially-available solvents.

Recently, low-dielectric-constant polymers have been put to use for diverse applications in the electronics industry, such as flexible circuitry substrates, stress buffers, interlayer dielectrics, and passivation layers. The development of low-dielectric-constant and thermostable polymers has been quite dramatic and has drawn the attention of many polymer scientists. Aromatic polyimides possess many useful properties and are increasingly being required by the electronic circuit industry [5, 12]. A low dielectric constant is one of the most attractive properties of polyimide materials for electronic applications. One of the most effective methods used to decrease the dielectric constant is to introduce fluorine atoms into polyimide materials [12]. As is well-known, the strong electronegativity of fluorine results in very low polarizability of the C–F bonds. In the past two to three decades, a number of fluorine-containing dianhydrides and diamines have been introduced to prepare fluorinated polyimides with low water uptake, low refractive index, and low dielectric constant, while maintaining many of advantages of polyimides. Fluorination is also known to enhance the solubility and optical transparency, and to lower moisture absorption of polyimides [13, 14, 15]. Therefore, it is expected that fluorinated polyimides will be widely applied in the electro-optical and semiconductor industries.

Recent studies demonstrated that polyimides derived from ether-bridged aromatic diamines with trifluoromethyl (3F) groups are soluble high temperature polymer materials with low moisture uptake, low dielectric constant, high optical transparency, and low birefringence [16, 17]. In our previous papers [18, 19, 20], we described how we successfully used the cyclic side cardo fluorene group-containing polyamides and polyimides derived from 9,9-bis [4-(4-aminophenoxy)phenyl]fluorene with various aromatic dicarboxylic acids and dianhydrides. We found that the incorporation of both ether and a fluorine group into the macromolecular backbone results in polymers with good thermal stability, high T_g, and improved solubility. In this study, a high-purity CF_3-containing diamine, 9,9-bis [4-(4-amino-2-trifluoromethylphenoxy)phenyl]fluorene (**II**), was synthesized through a modificatory method and subsequently polycondensed with various commercially-available aromatic dianhydrides to produce a series of fluorinated polyimides ($\mathbf{V_{a\text{-}f}}$). These polymers were subjected to solubility, moisture absorption, thermal, optical, and dielectric property measurements, and compared to analogous polyimides ($\mathbf{VI_{a\text{-}f}}$) prepared from a nonfluorinated diamine monomer, 9,9-bis [4-(4-aminophenoxy)phenyl]fluorene.

Experimental

Materials

9,9-bis(4-hydroxyphenyl)fluorene (BHPF, Acros) and 2-chloro-5-nitrobenzotrifluoride (Acros) were used as received. Pyromellitic dianhydride (PMDA or $\mathbf{III_a}$; Aldrich), 3,3′,4,4′-benzophenonetetracarboxylic dianhydride (BTDA or $\mathbf{III_b}$; Aldrich), diphenylsulfone-3,3′,4,4′-tetracarboxylic dianhydride (DSDA or $\mathbf{III_d}$; New Japan Chemical Co.), and 4,4′-oxydiphthalic dianhydride (ODPA or$\mathbf{III_c}$; Oxychem) were recrystallized from acetic anhydride before use. 3,3′,4,4′-biphenyltetracarboxylic dianhydride (BPDA or$\mathbf{III_c}$; Oxychem) and 2,2-bis(3,4-dicarboxyphenyl)hexafluoropropane dianhydride (6FDA or $\mathbf{III_f}$; Hoechst) were purified by sublimation. *N*-Methyl-2-pyrrolidone (NMP; Fluka), *N*,*N*-dimethylacetamide (DMAc; Fluka), *N*,*N*-dimethylformamide (DMF; Fluka), and pyridine (Py; Wako) were purified by distillation under reduced pressure over calcium hydride, and stored over 4 Å molecular sieves.

Synthesis of monomer

*9,9-bis[4-(4-nitro-2-trifluoromethylphenoxy)phenyl]fluorene (**I**)*

BHPF (11.32 g, 0.0323 mol) and 2-chloro-5-nitrobenzotrifluoride (14.62 g, 0.0648 mol) were first dissolved in 25 ml of DMAc in a 300 ml flask with stirring. After the mixture was completely dissolved, potassium carbonate (6.7 g, 0.048 mol) was added to it in one portion, and the mixture was heated at 110 °C for 12 h. The obtained mixture was poured into 100 ml of methanol/water (volume ratio 2/1) to give a yellow solid, which was collected, washed with water, and dried under vacuum. The crude product was recrystallized from DMF/methanol to give fine, white powder (22.36 g, 95%).

The properties of the product were found to be as follows. Melting point: 221–222 °C by differential scanning calorimetry (DSC) at a scan rate of 10 °C/min. IR (KBr): 1532, 1355 (–NO_2stretch), 1284, 1178, 1138, 1112 cm^{-1} (C–F and C–O stretch). ^1H NMR (DMSO-d_6, δ, ppm): 8.51, 8.50 (d, 2H, H_a), 8.43–8.46 (dd, 2H, H_b), 7.99, 7.98 (d, 2H, H_i), 7.54, 7.53 (d, 2H, H_f), 7.47, 7.46, 7.44 (t, 2H, H_h), 7.41, 7.39, 7.38 (t, 2H, H_g), 7.31, 7.29 (d, 4H, H_e), 7.18, 7.16 (d, 4H, H_d), 7.14, 7.12 (d, 2H, H_c). ^{13}C NMR (DMSO-d_6, δ, ppm): 159.8 (C^4), 152.6 (C^7), 150.0 (C^{11}), 143.1 (C^1), 141.7 (C^{10}), 139.5 (C^{16}), 130.1 (C^6), 129.9 (C^9), 128.1 (C^{12}), 128.0 (C^{15}), 126.0 (C^{13}), 123.3 (C^2, quartet, $^3J_{C\text{-}F} = 5$ Hz), 122.2 (C^{17}, quartet, $^1J_{C\text{-}F} = 271$ Hz), 120.7 (C^{14}), 120.2 (C^8), 118.9 (C^3, quartet, $^2J_{C\text{-}F} = 31$ Hz), 118.2 (C^5), 64.0 (C^{18}).

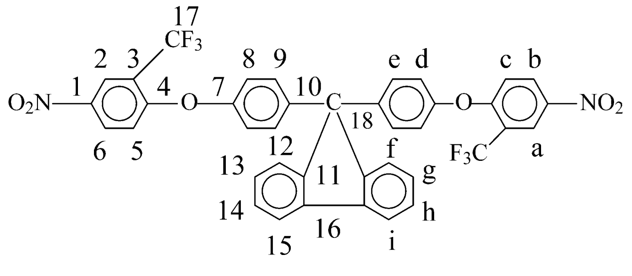

Calculated elemental analysis: for $C_{39}H_{22}F_6O_6N_2$ (728.6): C, 64.29%; H, 3.04%; N, 3.84%. Found: C, 64.22%; H, 2.98%; N, 3.81%.

*9,9-bis[4-(4-amino-2-trifluoromethylphenoxy)phenyl]fluorene (**II**)*

To a suspension solution of the purified dinitro compound **I** (20.06 g, 0.03 mol) and 10% Pd/C (0.2 g) in ethanol (150 ml), hydrazine monohydrate (7 ml) was added dropwise to the stirred mixture at 70–80 °C for 30 min. After complete addition, the mixture was heated at reflux temperature for another 2 h. The reaction solution was filtered hot to remove Pd/C, and the filtrate was then distilled to remove the solvent. The obtained mixture was poured into hot water to precipitate powder, that was dried in vacuum to give white crystals **II** (18.25 g, 91%).

The properties of the crystals were found to be as follows. Melting point: 239–240 °C by DSC (10 °C/min). IR (KBr): 3000–3500 (N–H stretch), 1272, 1232, 1160, 1132 cm^{-1} (C–O and C–F stretch). ^1H NMR (DMSO-d_6, δ, ppm): 7.93, 7.91 (d, 2H, H_i), 7.44, 7.43 (d, 2H, H_f), 7.41, 7.40, 7.38 (t, 2H, H_h), 7.33, 7.32, 7.30 (t, 2H, H_g), 7.08, 7.05 (d, 4H, H_e), 6.90 (d, 2H, H_a), 6.86, 6.84 (d, 2H, H_c), 6.80, 6.79 (d, 2H, H_b), 6.78, 6.76 (d, 4H, H_d), 5.44 (s, 4H, $-NH_2$). ^{13}C NMR (DMSO-d_6, δ, ppm): 157.0 (C^4), 150.7 (C^{11}), 145.7 (C^7), 142.1 (C^1), 139.4 (C^{10}), 139.3 (C^{16}), 128.9 (C^9), 127.8 (C^{12}), 127.6 (C^{15}), 125.9 (C^{13}), 123.4 (C^{17}, quartet, $^1J_{C\text{-}F} = 271$ Hz), 123.0 (C^6), 121.3 (C^3, quartet, $^2J_{C\text{-}F} = 31$ Hz), 120.4 (C^{14}), 118.5 (C^5), 116.3 (C^8), 110.5 (C^2, quartet, $^3J_{C\text{-}F} = 5$ Hz), 63.6 (C^{18}).

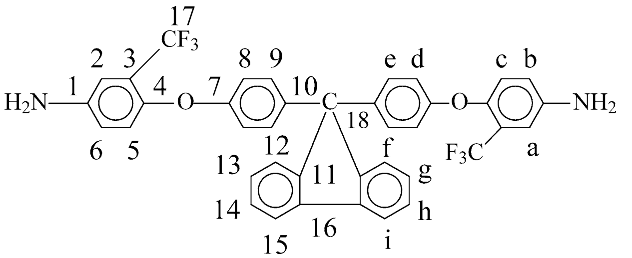

Calculated elemental analysis: for $C_{39}H_{26}F_6O_2\ N_2$ (668.64): C, 70.06%; H, 3.92%; N, 4.19%. Found: C, 70.02%; H, 3.89%; N, 4.17%.

Polymer synthesis

The general polymerization procedure is illustrated by the following example. Diamine **II** (0.668 g, 1 mmol) was dissolved in 6.9 ml of dried DMAc in a 50 mL flask. After the diamine was dissolved completely, 0.218 g (1 mmol) of PMDA **III$_a$** was added to it in one portion. The mixture was stirred at room temperature for 12 h to form a poly(amic acid) solution. Poly(amic acid) solution was then poured into a glass culture dish (diameter = 9 cm), which was placed in an 80 °C oven for 1 h to remove the solvent. The semi-dried poly(amic acid) film was further dried and imidized by sequential heating at 120 °C for 10 min, 150 °C for 10 min, 180 °C for 10 min, 210 °C for 10 min, and 250 °C for 30 min. By being soaked in water, a flexible polyimide film of **V$_a$** was self-stripped off from the glass surface. The inherent viscosity of **V$_a$** in DMAc at a 0.5 g/dL concentration at 30 °C was 1.02 dL/g (Table 1).

The IR absorption bands of the polymer film were found to be as follows: 1778, 1722 (imide C = O), 1378 (C–N stretch), 1095, 725 cm^{-1} (imide ring deformation). ^1H NMR (DMSO-d_6, δ, ppm): 8.39 (s, 2H, H_j), 7.97, 7.96 (d, 4H, H_a, H_i), 7.77, 7.75 (d, 2H, H_b), 7.52, 7.51 (d, 2H, H_f), 7.45, 7.44, 7.42 (t, 2H, H_h), 7.39, 7.37, 7.35 (t, 2H, H_g), 7.26, 7.24 (d, 4H, H_e), 7.22, 7.20 (d, 2H, H_c), 7.11, 7.09 (d, 4H, H_d). ^{13}C NMR (DMSO-d_6, δ, ppm): 165.2 (C^{21}), 154.2 (C^4), 154.0 (C^7), 150.2 (C^{11}), 141.9 (C^1), 139.4 (C^{10}), 137.0 (C^{20}), 133.3 (C^{16}), 129.6 (C^9), 128.0 (C^{12}), 127.8 (C^{15}), 126.3 (C^{19}), 125.9 (C^{13}), 124.2 (C^6), 122.9 (C^{17}, quartet, $^1J_{C\text{-}F} = 271$ Hz), 120.6 (C^{14}), 119.3 (C^5), 119.2 (C^8), 119.2 (C^3, quartet, $^2J_{C\text{-}F} = 31$ Hz), 117.9 (C^2), 63.9 (C^{18}).

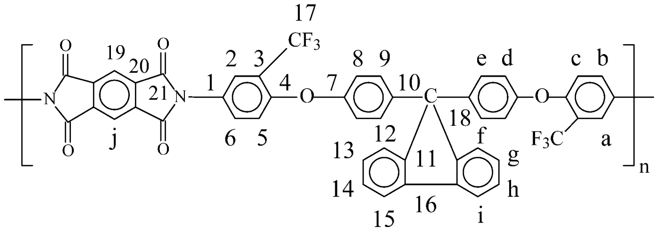

Measurements

IR spectra were recorded on a Horiba Fourier-Transform Infrared Spectrometer FT-720. Elemental analyses were run in a Perkin-Elmer Model 2400 C, H, N analyzer. ^1H and ^{13}C spectra were recorded on a Bruker AV-500 FT-NMR spectrometer. Inherent viscosities were determined at 0.5 g/dL concentration using a Cannon-Fenske viscometer at 30 °C. Thermogravimetry analysis (TGA) was conducted with a TA Instruments TGA 2050. Experiments were carried out on 9–11 mg film samples heated in flowing nitrogen or air (90 cm^3/min) at a heating rate of 20 °C/min. Differential scanning calorimeter (DSC) traces were measured on a TA Instruments DSC 2010 at the rate of 15 °C/min in flowing nitrogen (40 cm^3/min). Glass transition temperatures were read as the midpoint of the heat capacity jump and were taken from the second heating scan after a quick cool-down from 400 °C. Mechanical properties

Table 1 Inherent viscosity of poly(amic acid)s and polyimides, and elemental analysis of the polyimides

Poly(amic acid)		Polyimide		Formula	Elemental analysis (%)			
Code	η_{inh}(dL/g)[a]	Code	η_{inh}(dL/g)[a]	M_w	Calculated or experimentally found	C	H	N
IV$_a$	1.07	**V$_a$**	1.02	$(C_{49}H_{24}O_6N_2F_6)_n$	Calcd	69.18	2.84	3.29
				$(850.73)_n$	Found	69.11	2.81	3.27
IV$_b$	1.03	**V$_b$**	0.98	$(C_{56}H_{28}O_7N_2F_6)_n$	Calcd	70.44	2.96	2.93
				$(954.84)_n$	Found	70.46	2.98	2.96
IV$_c$	1.07	**V$_c$**	1.03	$(C_{55}H_{28}O_6N_2F_6)_n$	Calcd	71.28	3.05	3.02
				$(926.83)_n$	Found	71.32	3.09	3.05
IV$_d$	0.93	**V$_d$**	0.88	$(C_{55}H_{28}O_8N_2F_6S_1)_n$	Calcd	66.67	2.85	2.83
				$(990.89)_n$	Found	66.68	2.87	2.85
IV$_e$	0.96	**V$_e$**	0.92	$(C_{55}H_{28}O_7N_2F_6)_n$	Calcd	70.07	2.99	2.97
				$(942.83)_n$	Found	70.04	2.96	2.92
IV$_f$	0.90	**V$_f$**	0.84	$(C_{58}H_{28}O_6N_2F_{12})_n$	Calcd	64.69	2.62	2.60
				$(1076.85)_n$	Found	64.62	2.59	2.57

[a] Measured at a polymer concentration of 0.5 g/dL in DMAc at 30 °C

of the films were measured with an Instron model 1130 tensile tester with a 5 kg load cell at a crosshead speed of 5 cm/min on strips approximately 40–50 µm thick and 0.5 cm wide with a 2 cm gauge length. An average of at least five individual determinations was used. The color intensity of the polymers was evaluated with a Macbeth Color-eye colorimeter. Measurements were performed with films, using an observational angle of 10° and a CIE (Commission International de l'Eclairage)-D illuminant. A CIE LAB color difference equation was used. Ultraviolet-visible (UV-Vis) spectra of the polymer films were recorded on a Shimadzu UV-1601 UV-Vis spectrophotometer. The dielectric property of the polymer films was tested via the parallel-plate capacitor method with a Hewlett Packard 4194A dielectric analyzer. Gold electrodes were vacuum-deposited on both surfaces of dried films. Experiments were performed at 25 °C in a dry chamber. The equilibrium moisture absorption was determined by the weighing of the changes in vacuum-dried film specimens before and after immersion in deionized water at 25 °C for three days.

Results and discussion

Monomer synthesis

The 3F-containing bis(ether amine)**II** was prepared in two steps according to a well-developed method (Scheme 1) [16, 17]. The first step is a Williamson etherification reaction of BHPF and 2-chloro-5-nitrobenzotrifluoride in the presence of potassium carbonate in DMAc, followed by stirring of the mixture at 110 °C for 12 h. The diamine **II** was readily obtained in a good yield by the catalytic reduction of the intermediate dinitro compound **I** with hydrazine hydrate and Pd/C catalyst in refluxing ethanol. Because the reaction activity of 2-chloro-5-nitrobenzotrifluoride with bisphenol was higher than that of 1-chloro-4-nitrobenzene, both the reaction temperature and the amount of K_2CO_3 could be reduced to avoid coloring the dinitro compound. In this study, the reaction that proceeded at 100–110 °C for 8 h produced a better result. FTIR, NMR, and elemental analysis were used to confirm the structures of the intermediate**I** and the diamine monomer **II**. Figure 1 shows the FTIR spectra of dinitro compound **I** and diamine **II**. The nitro group of compound**I** gave two characteristic bands at 1532 and 1355 cm^{-1} (NO_2 asymmetric and symmetric stretching). After reduction, the characteristic absorptions of the nitro group disappeared, and the amino group showed the pair of N–H stretching bands in the region of 3300–3500 cm^{-1}.

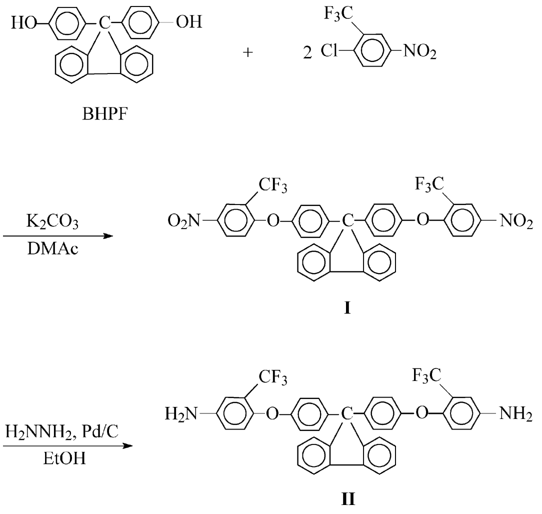

Scheme 1 Synthesis of 3F-diamine **II**

The absorption signals of aromatic protons of**I** appeared in the region of 7.1–8.6 ppm, and those of **II** shifted to the higher field between 6.7–8.0 ppm. In the ^{1}H NMR spectrum of **I**, the protons H_a and H_b

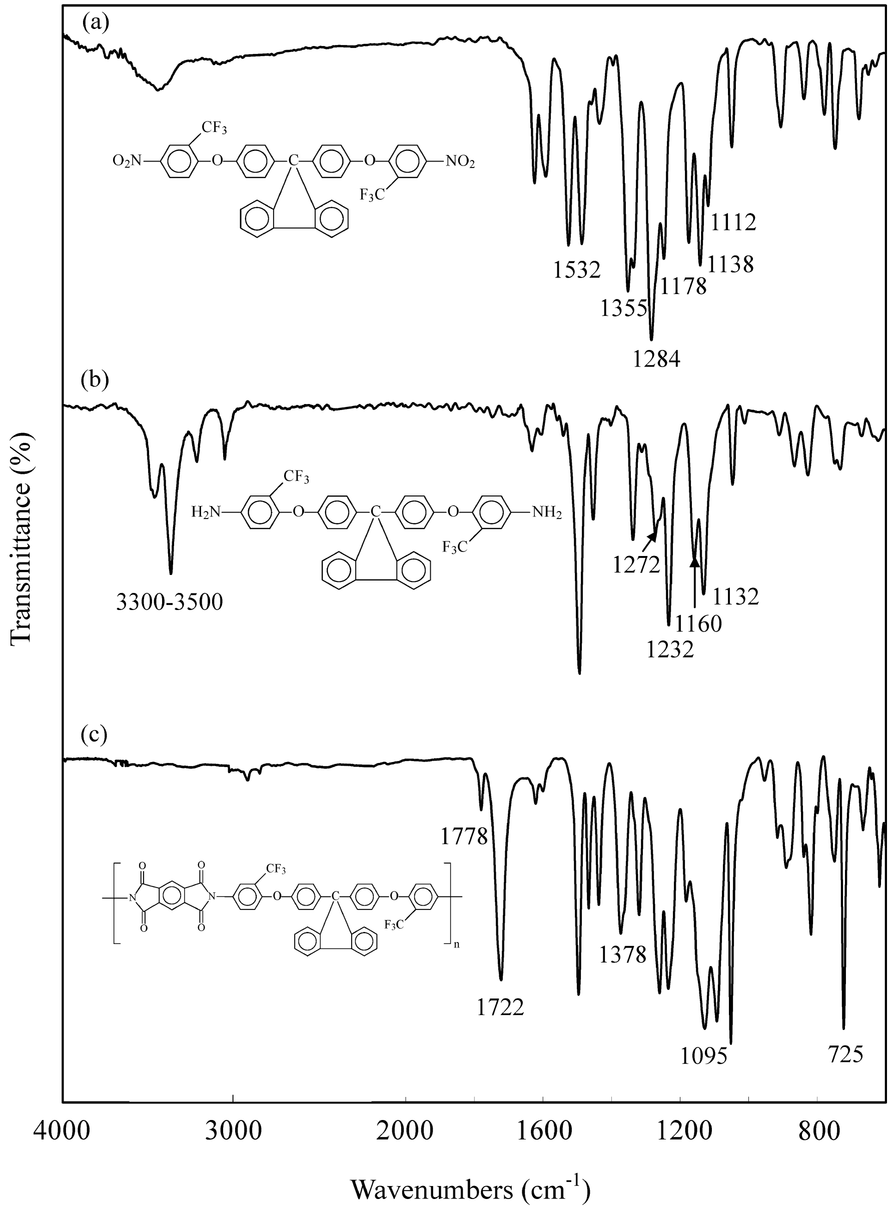

Fig. 1 FTIR spectra of **a** 3F-dibitro compound **I**, **b** 3F-diamine **II**, and **c** a representative polyimide$\mathbf{V_a}$

resonated at the farthest downfield region because of the inductive effect of electron withdrawing NO_2 and CF_3 groups; the H_d and H_c presented in the upfield shifting of their positions might be due to the electron-donating phenoxy groups in the ortho positions. After reduction, the protons $H_{f\text{-}i}$ adjacent to the fluorene group resonated at the farthest downfield region, as a result of the inductive effect and resonance; the H_b of **II** still resonated at the more downfield region on account of the inductive effect of the amino group. The chemical shifts of H_d presented in the upfield shifting of their positions might be due to the electron-donating phenoxy groups in the ortho positions.

In ^{13}C NMR spectra, all of the carbon-13 atoms in **I** and**II** showed 18 main signals in the region 63–160 ppm, including 16 signals of carbon from benzene and one signal of the C^{18} quaternary carbon. The ^{13}C NMR spectrum of **I** showed three quartets because of the heteronuclear ^{13}C–^{19}F coupling. The large quartet centered at about 122 ppm was due to the CF_3 carbon. The one-bond C–F coupling constant in this case was about 271 Hz. The CF_3-attached carbon (C^3) also showed a clear quartet centered at about 119 ppm, with a smaller coupling constant of about 31 Hz because of the two-bond C–F coupling. Besides, the C^2 carbon (ortho to the CF_3 group) also had its resonance split by the three fluorines (three-bond coupling). The close quartet had an even smaller coupling constant (ca. 5 Hz) because the interaction operated over more bonds. Similar splitting patterns (with $^1J_{C\text{–}F} = 271$ Hz, $^2J_{C\text{–}F} = 31$ Hz, and

$^3J_{C-F} = 5$ Hz) were also found in the ^{13}C NMR spectrum of **II**. All of the spectroscopic data obtained were in good agreement with the expected structures.

Polymer synthesis

All of the polymers **V** were synthesized from diamine **II** and dianhydrides **III$_{a\text{-}f}$**, by following a conventional two-step procedure before the ring-opening polyaddition at room temperature to poly(amic acid)s **IV**, followed by sequential heating to 250 °C to obtain the corresponding polyimides, as shown in Scheme 2. Figure 2 presents the variation curves of inherent viscosities of the poly(amic acid)s obtained from PMDA with CF_3-containing diamine **II** or nonfluorinated**VI** at various times. The reaction of PMDA with fluorinated **II** proceeded relatively slowly and its inherent viscosity reached 0.8 dL/g after 3 h. After this point, inherent viscosity increased slowly; polymerization nearly ceased and no increase in inherent viscosity (1.07 dL/g) was observed after 10 h. The reaction of PMDA with **II′** proceeded relatively quickly and its inherent viscosity increased rapidly within 60 min; inherent viscosity reached 1.21 dL/g after 80 min and then decreased gradually.

IR spectroscopy allowed monitoring of the imide ring formation during thermal curing. The typical set of

Scheme 2 Synthesis of the polyimides

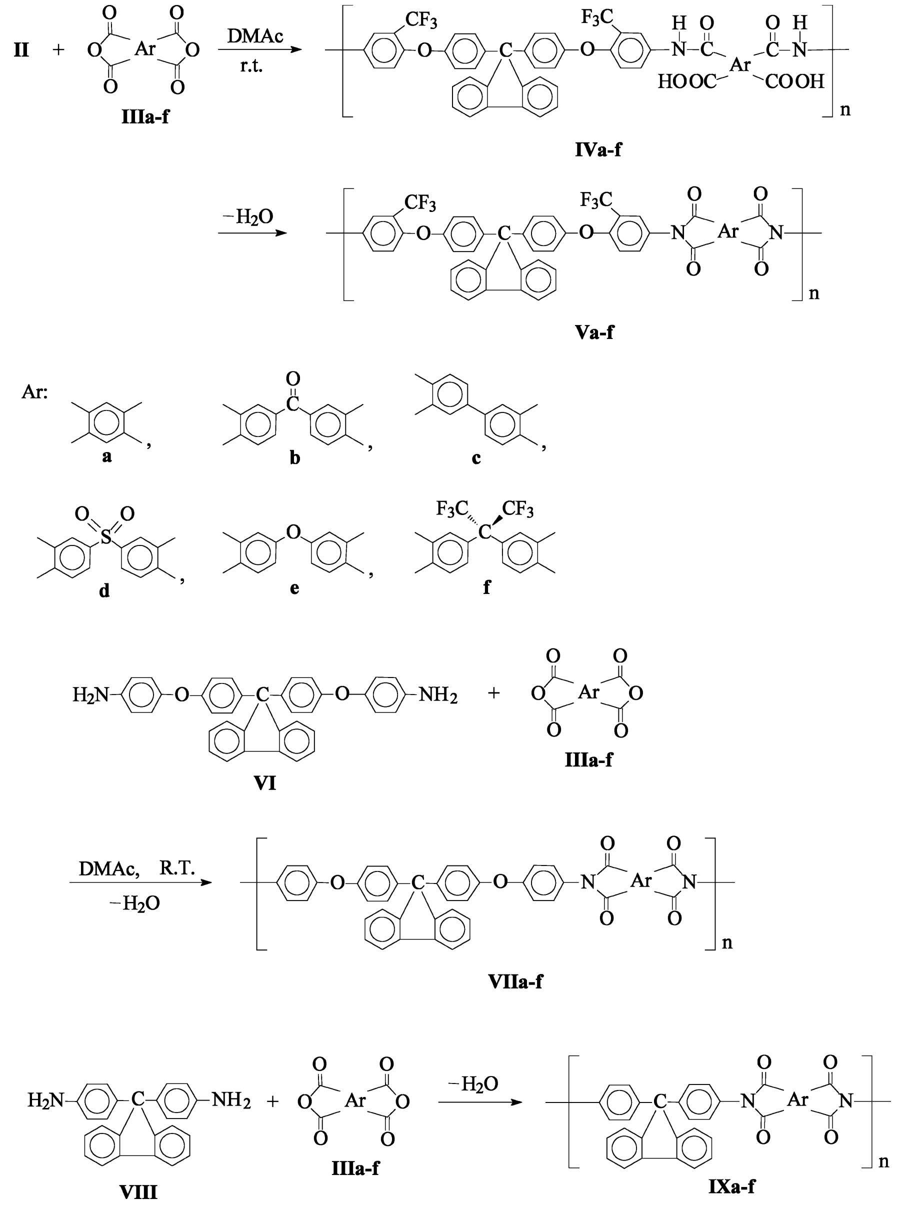

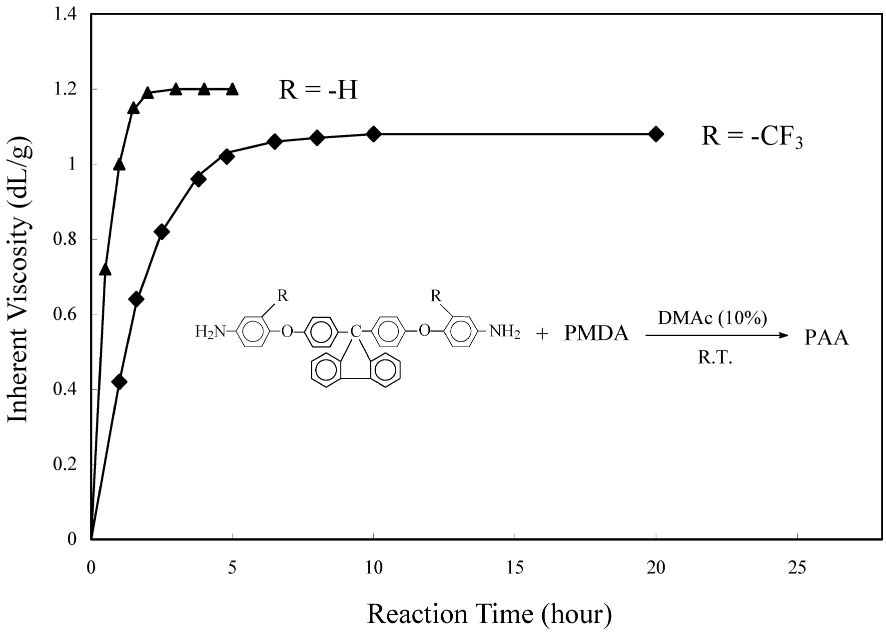

Fig. 2 Viscosity change of poly(amic acid)s prepared in DMAc at 10% solid content at room temperature

FTIR spectra of polyimide $\mathbf{V_a}$ are shown in Fig. 1. As the poly(amic acid) was converted into the polyimide, the characteristic absorption bands of the imide ring were observed near 1778 and 1722 (asymmetrical and symmetrical C = O stretching vibration), 1378 (C–N stretching vibration), and 1095 and 725 cm^{-1} (imide ring deformation), together with some strong absorption bands in the region of 1100–1300 cm^{-1} because of the C–O and C–F stretching. The disappearance of amide and carboxyl bands indicates a virtually complete conversion of the poly(amic acid) precursor into polyimide.

In general, structure identification of standard aromatic polyimides via NMR spectroscopy is difficult because of poor solubility. In this study, polyimides **V** had good solubility in organic solvent and could be easily identified by NMR spectra. The typical NMR spectra of soluble polypyromellitimide$\mathbf{V_a}$ are shown in Fig. 3. In the ^{1}H NMR spectrum, all of the protons resonated in the region of 7.0–8.4 ppm. The protons $H_j$on the pyromellitimide unit resonated farthest downfield, on account of the inductive effect and resonance. H_a also resonated at the lower field because of its closeness to the electron-withdrawing CF_3 group and imide ring. The $H_c$and H_d shifted to higher field due to the electron-donating property of aromatic ether. The ^{13}C NMR spectrum of $\mathbf{V_a}$ exhibited 21 signals in the range of 63–166 ppm, including one signal of carbon C^{21} of the carbonyl group, 16 signals of carbon from benzene and one signal from the C^{18} quaternary carbon. Furthermore, the splitting of the ^{13}C signals caused by couplings between carbon and fluorine could also be observed in the spectrum. The magnitudes of the one-bond and two-bond carbon-fluorine couplings $^1J_{CF}$ and $^2J_{CF}$ were 271 Hz and 31 Hz, respectively. The results of elemental analysis of$\mathbf{V_{a\text{-}f}}$ are listed in Table 1. The above-cited results show that series **V** has been synthesized successfully.

Properties of polymers

The solubilities of these polyimides were tested in various organic solvents, and the results are summarized in Table 2. The series of polymers**V** have excellent solubilities in aprotic polar solvents such as NMP, DMAc, DMF, and DMSO, and are also soluble in less polar solvents like *m*-cresol, pyridine, and dioxane. The good solubility of polyimides **V** might be due to the presence of bulky fluorene and CF_3 groups in the diamine moiety. Compared with polyimides **VII** and **IX**, polyimides **V** show better solubility. This difference in solubility might be attributed to the molecular asymmetry and the presence of bulky trifluoromethyl groups, which increase the disorder in the chains and hinder dense chain stacking, thereby reducing the interchain interactions and so enhancing solubility.

The color intensities of the polyimides were elucidated from the yellowness or redness indices observed by a Macbeth color-eye colorimeter. For comparison, the corresponding polyimides**VII** and **IX** without the CF_3 groups were also prepared and characterized by their color intensity. The color coordinates of these polyimides are given in Table 3. The color intensity of polyimides is affected by dianhydride moieties, and decreases in the following order: PMDA > BTDA > DSDA > BPDA > ODPA > 6FDA. $\mathbf{V_{c\text{-}f}}$ displayed

Fig. 3 The ^1H and ^{13}C NMR spectra of polyimide $\mathbf{V_a}$ in DMSO-d_6

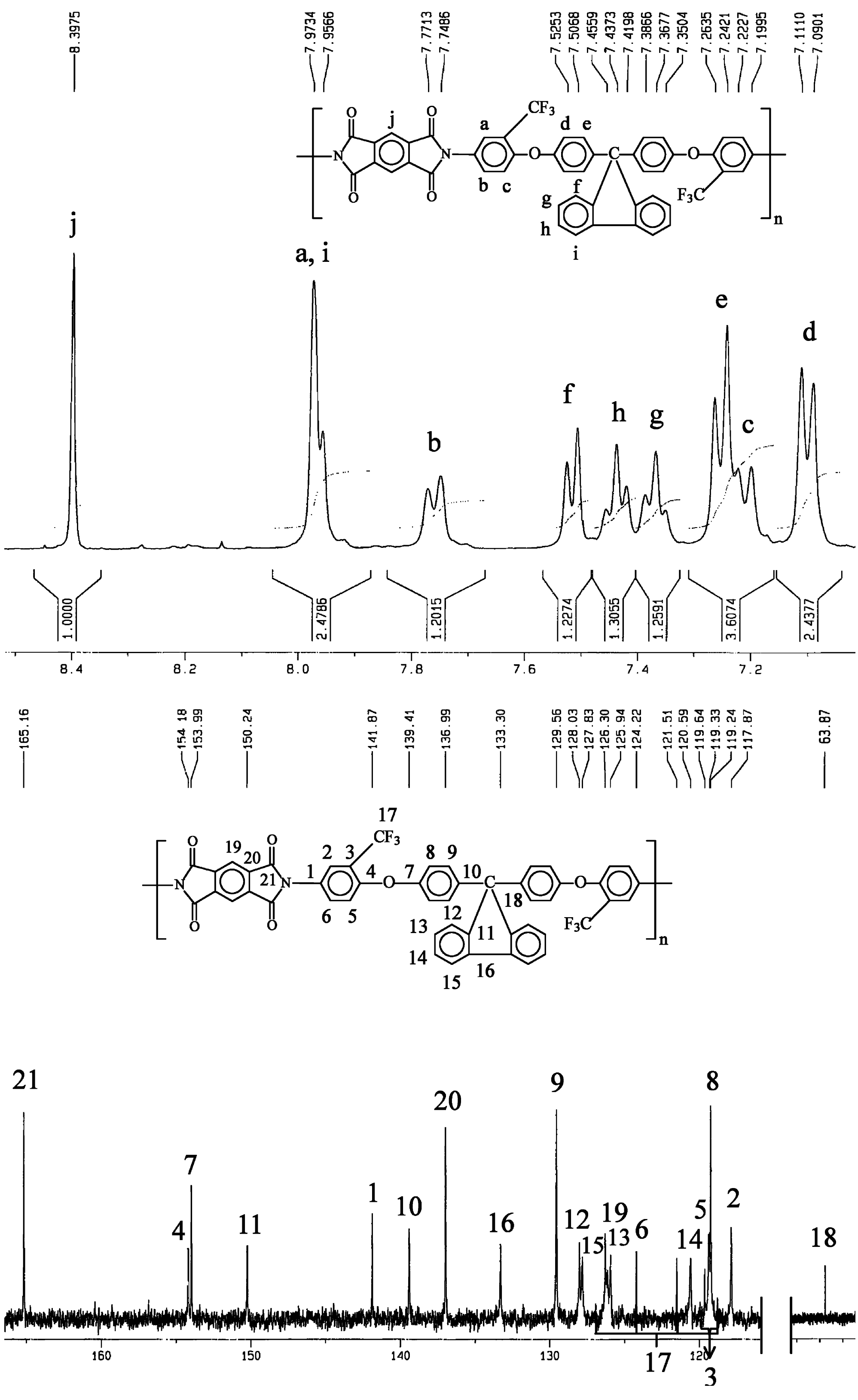

Table 2 Solubility behavior of the polyimides[a]

Polymer	Solvent[c]						
	NMP	DMAc[b]	DMF	DMSO	Py	*m*-Cresol	dioxane
$\mathbf{V_a}$	+ +	(+ +)	+ +	+ +	+ +	+ +	+ +
$\mathbf{V_b}$	+ +	(+ +)	+ +	+	+ +	+	+
$\mathbf{V_c}$	+ +	(+ +)	+ +	+ +	+ +	+ +	+ +
$\mathbf{V_d}$	+ +	(+ +)	+ +	+ +	+ +	+ +	+ +
$\mathbf{V_e}$	+ +	(+ +)	+ +	+ +	+ +	+ +	+ +
$\mathbf{V_f}$	+ +	(+ +)	+ +	+ +	+ +	+ +	+ +
$\mathbf{VII_a}$	-	-	-	-	-	-	-
$\mathbf{VII_b}$	-	-	-	-	-	-	-
$\mathbf{VII_c}$	-	-	-	-	-	-	-
$\mathbf{VII_d}$	-	-	-	-	-	-	-
$\mathbf{VII_e}$	+	+	-	-	S	-	-
$\mathbf{VII_f}$	+ +	+ +	+	+	+	+	-
$\mathbf{IX_a}$	-	-	-	-	-	-	-
$\mathbf{IX_b}$	-	-	-	-	-	-	-
$\mathbf{IX_c}$	-	-	-	-	-	-	-
$\mathbf{IX_d}$	-	-	-	-	-	-	-
$\mathbf{IX_e}$	+	+	-	-	-	-	-
$\mathbf{IX_f}$	+	+	+	S	+	+	-

[a] Qualitative solubility was determined with 10 mg of polymer in 1 ml of solvent: + +, soluble at room temperature; +, soluble on heating; S, swelling or partially soluble; -, insoluble even on heating. [b] The solubility was determined at 10% solid content. [c] NMP: *N*-methyl-2-pyrrolidone; DMAc:*N,N*-dimethylacetamide; DMF:*N,N*-dimethylformamide; DMSO: dimethyl sulfoxide; Py: pyridine; THF: tetrahydrofuran

Table 3 Color coordinates and cut-off wavelength (λ_0) from UV-Vis spectra for both **V**,**VI** and **IX** series polyimide films

Polymer	Code[a]			$\lambda_{\text{cut-off}}$(nm)[b]	Film thickness (μm)
	b^*	a^*	L^*		
Paper	−0.009	0.025	100	-	-
$\mathbf{V_a}$	50.4	−10.5	93.6	390	34
$\mathbf{V_b}$	35.9	−9.8	94.5	389	31
$\mathbf{V_c}$	12.1	−6.7	96.0	378	37
$\mathbf{V_d}$	21.2	−7.4	95.3	385	35
$\mathbf{V_e}$	8.4	−4.3	95.8	362	40
$\mathbf{V_f}$	6.1	−3.2	96.1	348	38
$\mathbf{VII_a}$	68.7	−6.8	90.2	418	42
$\mathbf{VII_b}$	65.3	−5.7	90.8	413	41
$\mathbf{VII_c}$	36.8	−4.4	93.8	401	43
$\mathbf{VII_d}$	41.4	−5.3	93.6	409	46
$\mathbf{VII_e}$	28.8	−3.8	93.7	388	48
$\mathbf{VII_f}$	22.6	−3.4	91.1	385	40
$\mathbf{IX_a}$	71.2	−5.8	86.4	421	40
$\mathbf{IX_b}$	67.6	−9.1	87.4	413	33
$\mathbf{IX_c}$	39.8	−10.9	90.5	404	38
$\mathbf{IX_d}$	45.8	−8.5	89.7	410	41
$\mathbf{IX_e}$	32.8	−9.5	90.0	394	42
$\mathbf{IX_f}$	25.9	−6.6	90.7	390	40
Kapton	85.1	0.3	90.1	443	38

[a] The color parameters were calculated according to a CIE LAB equation, using paper as a standard. L^* is lightness; 100 means white, while 0 implies black. A positive a^* means a red color, while a negative a^* indicates a green color. A positive b^* means a yellow color, while a negative b^* implies a blue color. [b] Transparency cut-off wavelength in nm

lighter color than the others. A comparison of series **V** polymers with series **VII** and **IX** polymers showed that the **V** series polyimides had a lower b^* value (yellowness index) than the corresponding polyimides **VII** and **IX**.

Moreover, the color intensities of the polyimides could also be elucidated from the cut-off wavelength observed in the UV-Vis absorption spectra. Figure 4 shows the UV-Vis spectra of the polyimide films, and the cut-off wavelengths from these spectra are listed in Table 3. Polyimides **V** had cut-off wavelengths in the range of 348–390 nm. $\mathbf{V_{c\text{-}f}}$ were lightly colored and exhibited cut-offs at wavelength shorter than 385 nm. In particular, 6FDA and ODPA produced fairly transparent and almost colorless polyimide films in contrast to other dianhydrides. Consistent with the results obtained from the colorimeter, all of the fluorinated polyimides

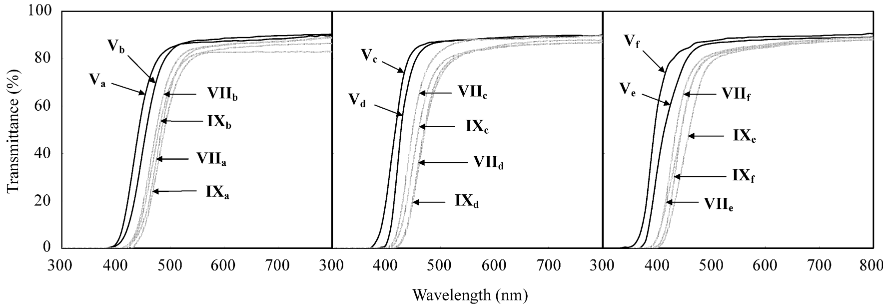

Fig. 4 UV-visible spectra of polyimide films

Table 4 Tensile properties of polyimide films

Polymer	Strength at break (MPa)	Elongation at break (%)	Initial modulus (GPa)
$\mathbf{V_a}$	97	8	2.18
$\mathbf{V_b}$	87	7	2.32
$\mathbf{V_c}$	105	9	2.42
$\mathbf{V_d}$	94	8	2.38
$\mathbf{V_e}$	98	9	2.23
$\mathbf{V_f}$	85	7	2.13
$\mathbf{VII_a}$	70	4	2.02
$\mathbf{VII_b}$	72	5	2.24
$\mathbf{VII_c}$	89	6	2.36
$\mathbf{VII_d}$	86	4	2.33
$\mathbf{VII_e}$	80	7	2.07
$\mathbf{VII_f}$	75	5	2.01

revealed a shorter cut-off wavelength than their respective nonfluorinated analogues. These results might be attributed to the reduction of the intermolecular charge transfer complex (CTC) between alternating electron-donor (diamine) and electron-acceptor (dianhydride) moieties. The light color of the polyimides with the CF_3groups in their diamine moieties may be explained from the decreased intermolecular interactions. The bulky and electron-withdrawing CF_3 group in diamine **II** is effective in decreasing CTC formation between polymer chains through steric hindrance and the inductive effect (by decreasing the electron-donating property of diamine moieties). A secondary positive effect of the 3F substituents on the film transparency is the weakened intermolecular cohesive force because of the lower polarizability of the C–F bond. The decrease of intermolecular CTC formation is also understandable from the significant solubility of the polyimides prepared from 3F-diamine **II**.

With the exception of the brittle behavior of polymer **IX,** all of the polyimides $\mathbf{V_{a\text{-}f}}$ could afford good quality and creasable films. These films were subjected to a tensile test, and their tensile properties are summarized in Table 4. The films had strengths at break of 83–105 MPa, elongations at break of 7–9%, and initial modulus of 2.13–2.42 GPa. On comparing mechanical properties of polymers **V** with their corresponding polymers **VII**, series **V** polymers showed good film-forming ability.

DSC and TGA were used to evaluate the thermal properties of the polymers. The thermal behavior data of all of the fluorinated polymers are presented in Table 5. Rapid cooling from 400 °C to room temperature produced predominantly amorphous samples, so the glass transition temperatures (T_g) of all the polyimides could be easily read in the subsequent heating DSC traces. The T_g values of polyimides $\mathbf{V_{a\text{-}f}}$ were in the range of 277–331 °C. Depending on the structure of the dianhydride

Table 5 Thermal behavior data for the polyimides

Polymer	DSC	TGA		
		Decomposition temp.[b] (°C)		Char yield[c]
	T_g[a](°C)	In air	In nitrogen	Wt%
$\mathbf{V_a}$	331	565	583	55
$\mathbf{V_b}$	285	576	594	59
$\mathbf{V_c}$	302	580	601	65
$\mathbf{V_d}$	299	544	552	60
$\mathbf{V_e}$	277	574	597	64
$\mathbf{V_f}$	292	554	564	56

[a] Midpoint of baseline shift in the second heating DSC trace with a heating rate of 15 °C/min under a nitrogen atmosphere. [b] Temperatures at which 5% and 10% weight loss were recorded by TG at a heating rate of 20 °C/min. [c] Residual weight % at 800 °C under a nitrogen atmosphere

Table 6 Moisture absorption and dielectric constants of the polyimides

Polyimide	Film thickness (μm)	Moisture absorption (%)	Dielectric constant[a]			
			1 kHz	10 kHz	1 MHz	40 MHz
$\mathbf{V_a}$	35	0.14	2.93	2.85	2.81	2.77
$\mathbf{V_b}$	34	0.24	2.98	2.90	2.85	2.80
$\mathbf{V_c}$	37	0.17	2.88	2.82	2.76	2.72
$\mathbf{V_d}$	36	0.22	2.95	2.86	2.83	2.78
$\mathbf{V_e}$	38	0.20	2.82	2.77	2.72	2.70
$\mathbf{V_f}$	33	0.12	2.78	2.74	2.68	2.62
$\mathbf{VII_a}$	37	0.27	3.29	3.23	3.17	3.11
$\mathbf{VII_b}$	36	0.35	3.34	3.27	3.22	3.15
$\mathbf{VII_c}$	37	0.28	3.23	3.15	3.09	3.04
$\mathbf{VII_d}$	32	0.33	3.26	3.19	3.12	3.07
$\mathbf{VII_e}$	35	0.29	3.16	3.12	3.04	2.98
$\mathbf{VII_f}$	31	0.21	3.11	3.05	2.96	2.90
Kapton[b]	40	0.42	3.89	3.85	3.80	3.75

[a] Measured by DEA at room temperature (dry dielectric constant).

[b] A reference polyimide prepared from PMDA and 4,4′-oxydianiline (η_{inh} of the poly(amic acid) precursor 1.90 dL/g)

component, T_g decreased with the increasing flexibility of the polymer backbones. As expected, the polyimide $\mathbf{V_a}$ derived from PMDA exhibited the highest T_g as a result of the rigid pyromellitimide unit. However, the polyimide $\mathbf{V_e}$ obtained from ODPA showed the lowest T_g of 277 °C. This is reasonable because its dianhydride moiety has a flexible ether linkage.

The thermal stability of the polyimides was evaluated by TGA conducted at a heating rate of 20 °C/min. The temperatures of 5% weight loss (T_5), 10% weight loss (T_{10}) in nitrogen and air atmospheres were determined from original TGA thermograms and are also tabulated in Table 5. The T_5 values of polyimides $\mathbf{V_{a\text{-}f}}$ stayed in the range of 552–601 °C in nitrogen and 544–580°C in air, respectively. They left more than 55% char yield at 800 °C in nitrogen. BPDA-derived$\mathbf{V_c}$ had the highest T_{10} and char yield.

The measurements of the dielectric constants were performed between gold layers: the polymer film was dried carefully, and a thin gold layer was vacuum-deposited on both surfaces of the film. This procedure excluded any contact problems. Table 6 shows the results. Fluorinated polyimides$\mathbf{V_{a\text{-}f}}$ had lower dielectric constants (2.68-2.85 at 1 MHz) than commercial polyimides such as Kapton films (3.8 at 1 MHz) and nonfluorinated polyimides $\mathbf{VII_{a\text{-}f}}$ (2.98–3.43 at 1 MHz). The decreased dielectric constants might be attributable to the presence of bulky fluorene and CF_3 groups in the diamine moiety, which resulted in less efficient chain packing and increased free volume. In addition, the strong electronegativity of fluorine resulted in very low polarizability of the C–F bonds, thereby decreasing the dielectric constant. Hence, the 6FDA-derived polyimide $\mathbf{V_f}$ exhibited the lowest dielectric constant among those prepared from the other dianhydrides of polyimides $\mathbf{V_{a\text{-}e}}$.

The moisture absorptions of series$\mathbf{V}$ are summarized in Table 6. In comparison, polyimides $\mathbf{V_{a\text{-}f}}$ exhibited lower moisture absorptions (0.12–0.24%) than the corresponding nonfluorinated homologues $\mathbf{VII_{a\text{-}f}}$ (0.21–0.35%) or the Kapton film (0.42%) did, because of the hydrophobicity of the CF_3 group. Moreover, polyimides $\mathbf{V_f}$ and $\mathbf{VII_f}$ exhibited the lowest moisture absorption on account of the higher fluorine content in the repeating unit.

Conclusions

A high-purity, colorless fluorinated diamine **II**, 9,9-bis[4-(4-amino-2-trifluoromethylphenoxy)phenyl]fluorene, was prepared through nucleophilic substitution reaction of 9,9-bis(4-hydroxyphenyl)fluorene and 2-chloro-5-nitrobenzotrifluoride, followed by catalytic reduction with hydrazine. A series of light-colored and organosoluble polyimides**V** were obtained from the trifluoromethyl-substituted diamine with different aromatic dianhydrides. These polyimides are characterized by excellent thermal stability and good mechanical properties. They exhibit better solubility, lighter color, lower dielectric constant, and lower moisture absorption than corresponding nonfluorinated polyimides.

Acknowledgements The authors are grateful to the National Science Council of the Republic of China for the support of this work (Grant NSC 91-2216-E-036-008).

References

1. Feger C, Khojasteh MM, Htoo MS (eds)(1993) Advances in polyimide science and technology. Technomic, Lancaster, UK
2. Abadie MJM, Sillion B (eds)(1991) Polyimides and other high-temperature polymers. Elsevier, Amsterdam
3. Mittal KL (ed)(1984) Polyimides: synthesis, characterization, and application, vols I,II. Plenum, New York
4. Feger C, Khojasteh MM, McGrath JE (eds)(1989) Polyimides: materials, chemistry, and characterization. Elsevier, Amsterdam
5. Wilson D, Stenzenberger HD, Hergenrother PM (eds)(1990) Polyimides. Chapman and Hall, New York
6. Cassidy PE (1980) Thermally stable polymers. Marcel Dekker, New York
7. Yang HH (1989) Aromatic high-strength fibers. Wiley, New York
8. Dupont BS, Bilow N, U. S. Pat. 1986;4592925, and Landis AL, Naselow AB, U. S. Pat. 1987;4645824
9. Higashi K, Noda Y, Eur. Pat. 1986;240249, and Tamai S, Ohta M, Kawashima S, Oikawa H, Ohkoshi K, Yamaguchi A, Eur. Pat. 1987;234882
10. Matsuura T, Ando S, Sasaki S, Yamamoto F (1993) Electron Lett 29:2107
11. Ando S, Sawada T, Inoue Y (1993) Electron Lett 29:2143
12. Ghosh MK, Mittal KL (eds)(1996) Polyimides: fundamentals and applications. Marcel Dekker, New York
13. Li F, Fang S, Ge JJ, Honigfort PS, Chen JC, Harris FW, Cheng SZD (1999) Polymer 40:4571
14. Li F, Ge JJ, Honigfort PS, Fang S, Chen JC, Harris FW, Cheng SZD (1999) Polymer 40:4987
15. Wang CS, Yang RW (1997) J Appl Polym Sci 66:609
16. Yang CP, Hsiao SH, Hsu MF (2002) J Polym Sci A1 40:524
17. Xie K, Zhang SY, Liu JG, He MH, Yang SY (2001) J Polym Sci A1 39:2581
18. Yang CP, Lin JH (1993) J Polym Sci A1 31:2153
19. Hsiao SH, Yang CP, Lin WL (1999) Macromol Chem Physic 200:1428
20. Yang CP, Lin JH (1996) In: Salamone JC (ed) Polymeric materials encyclopedia, vol 9. CRC, Boca Raton, pp 6214